Journal of Electrical and Computer Engineering Innovations
(JECEI)
Journal homepage: http://www.jecei.sru.ac.ir

Research paper

A New Low-Stress Boost Converter with Soft-Switching and Using Coupled-Inductor Active Auxiliary Circuit

M. A. Latifzadeh[1], P. Amiri[2,*], H. Allahyari[3], H. Faezi[1]

[1]*Faculty of Electrical and Computer Engineering, Malek-Ashtar University of Technology, Tehran Iran.*

[2]*Faculty of Electrical Engineering, Shahid Rajaee Teacher Training University, Tehran, Iran.*

[3]*Department of Electrical Engineering, K. N. Toosi University of Technology, Tehran, Iran.*

Article Info

Article History:
Received 28 January 2023
Reviewed 17 March 2023
Revised 06 April 2023
Accepted 15 May 2023

Keywords:
Boost converter
ZVS soft-switching
DC/DC converter
PWM converter

*Corresponding Author's Email Address: *pamiri@sru.ac.ir*

Abstract

Background and Objectives: Many applications use boost converters as front-end circuits, including power factor correction (PFC), solar power generation, fuel cell power conversion, battery chargers, and uninterruptible power supply. In addition, boost converters have a simple structure with low component counts, which makes them a convenient choice.

Methods: This article proposes a coupled-inductor active auxiliary circuit to create a new low-stress boost converter with soft-switching. The proposed auxiliary circuit supplies the main switch and diode with soft-switching ZVC turn-on and ZCS turn-off states. The main switch and diode are not deal with any extra stress of voltage or current. Furthermore, the soft switching condition is also provided for auxiliary circuit components.

Results: The proposed auxiliary circuit also has a simple structure, low circulating current losses, low cost, and simplicity in control. The operation state and performance of the proposed soft-switching boost converter are examined, and the design procedure is presented. Finally, a 200W prototype is implemented and tested to validate the theoretical results. The offered experimental data verified the theoretical analysis.

Conclusion: This paper provides a new low-stress soft-switching boost converter using a simple coupled-inductor in the auxiliary circuit. Moreover, the auxiliary part consists of two diodes, one switch, one resonance capacitor, and a coupled inductor. The suggested auxiliary circuit provides soft switching condition for the main switch, which provides ZVS in the turn-on transient and ZCS in the turn-off transient, while in this situation, the soft-switching condition is provided for the auxiliary switch, which turns on under ZCS and also turns off with practically ZVS conditions. The auxiliary circuit does not impose additional voltage or current stress on the main switch. A 200 W prototype is implemented to validate the performance of this snubber cell. The experimental data reported here support the theoretical analysis. The best point of efficiency is 95.9% which is occurred at maximum load, and is 6.3% greater than the traditional counterparts.

This work is distributed under the CC BY license (http://creativecommons.org/licenses/by/4.0/)

Introduction

Many applications use boost converters as front-end circuits, including power factor correction (PFC), solar power generation, uninterruptible power supply (UPS), fuel cell power conversion, battery chargers, and car high-intensity discharge (HID) headlamps [1]-[7]. Regarding

boost, converters have a simple structure with low component counts, straightforward to implement, design, and control [8]-[10]. However, the main switch of a boost converter is hard switched, and switching losses and reverse recovery problems of the diode limit the efficiency, power density, and switching frequency. Furthermore, hard switching intensifies electromagnetic interferences (EMI) [11]-[13]. On the other hand, by introducing and developing soft-switching techniques which remove switching losses, these converters can operate at high switching frequencies. The significant advantages of a soft-switching converter are small size, lightweight, low EMI, and high-power density [14]-[15]. Meanwhile, soft-switching PWM converters, like PWM hard-switching converters, use a simple control circuit to design and experiment.

Recently, many passive and active auxiliary circuits have been proposed for the boost converter [16]-[30]. Although passive auxiliary circuits do not need any auxiliary switches and have a simple control method, their construction is typically complex and causes extra voltage and also current stress over the switch and diode of the converter [16]-[19]. Furthermore, this solution can only provide a turn-on ZCS condition and cannot recover capacitive turn-on losses. On the other hand, the active auxiliary circuits are proposed in [20]-[21] provide soft switching conditions for both the main switch and the main diode, although they operate with additional current stress on the main switch. The converter proposed in [22] provides the ZCS condition for the main switch. The primary switch voltage stress is increased in [23]-[24] by the series inductor that is used in the power path. In [25], the soft switching condition is achieved by way of having two auxiliary switches and increasing the converter's cost. [26]-[29] suggest an auxiliary circuit with a large number of components to decrease the current and voltage stress on the primary switch, however this increases cost and lowers efficiency and reliability. Higher conduction losses are caused by [20]-[22] and [25]-[29]'s significant circulation current losses and current stress through the auxiliary switches. The auxiliary switch in [30] also functions when being stressed by high voltage.

In this research, a novel coupled-inductor auxiliary circuit-based low stress soft-switching boost converter is suggested. The recommended auxiliary circuit corrects the issues listed above. The recommended auxiliary circuit turns on and off the main switch and main diode in ZVS and ZCS scenarios. Additionally, when ZCS requirements are met, the auxiliary switch activates, and when switching losses are minimal, it deactivates. The primary switch or main diode are not subjected to any additional current or voltage stress from the suggested auxiliary circuit. The recommended auxiliary circuit also features a straightforward design, little circulating current, and low losses.

Operating Statuses and Performance Analysis

Fig. 1 depicts the schematic of the proposed converter. Generally, this converter is divided into two sections: a) the boost converter and b) the auxiliary circuit. The input inductor L_1, the main switch S, the output capacitor C_o, and the main diode D_o comprise the boost converter.

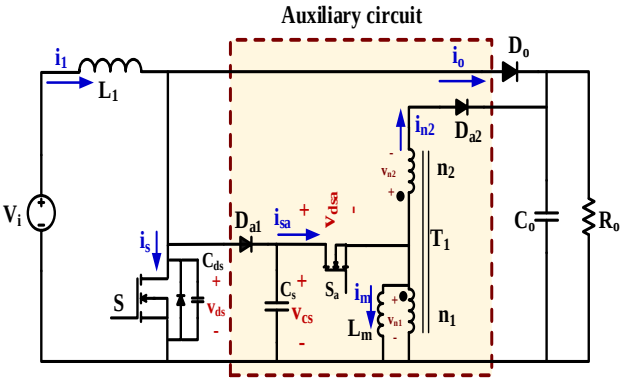

Fig. 1: The schematic of the proposed converter.

The auxiliary circuit is made up of the following components: the auxiliary input diode D_{a1}, the auxiliary capacitor C_s, the auxiliary switch S_a, the coupled inductors T_1, and the auxiliary output diode D_{a2}. T_1 is modeled by an ideal transformer with the turns ratio n_1: n_2 and magnetic inductance L_m, as shown in Fig. 1. Furthermore, C_{ds} is the drain-source parasitic capacitance of the primary switch S. The following assumptions simplify the analysis of the proposed circuit:

- The suggested converter works in a steady-state mode.
- Because the output capacitor C_o and the input inductor L_1 are both large enough, the output capacitor voltage and the input inductor current will be constant over a switching cycle.
- it was supposed that all components of this converter operate without losses, with the exception of the drain-source capacitance of the main switch.

During each switching cycle, seven operating states are identified to illustrate the operating principle of the suggested boost converter. Fig. 2 depicts the corresponding sub-intervals of the proposed structure. The key waveforms of the operational states are also illustrated in Fig. 3. The voltage is expected to be the same as the output voltage Vo before the initial status.

Operating Statuses

Status 1 [t0, t1]: Previous to this status, D_0 is conducting and S is turned off. This mode is initiated by applying the gate signal to the auxiliary switch S_a, and it is turned on under ZCS conditions. When the output voltage is applied across the magnetizing inductor of the L_m, the current i_m increases linearly to I_b, and the current I_{Do} falls linearly to

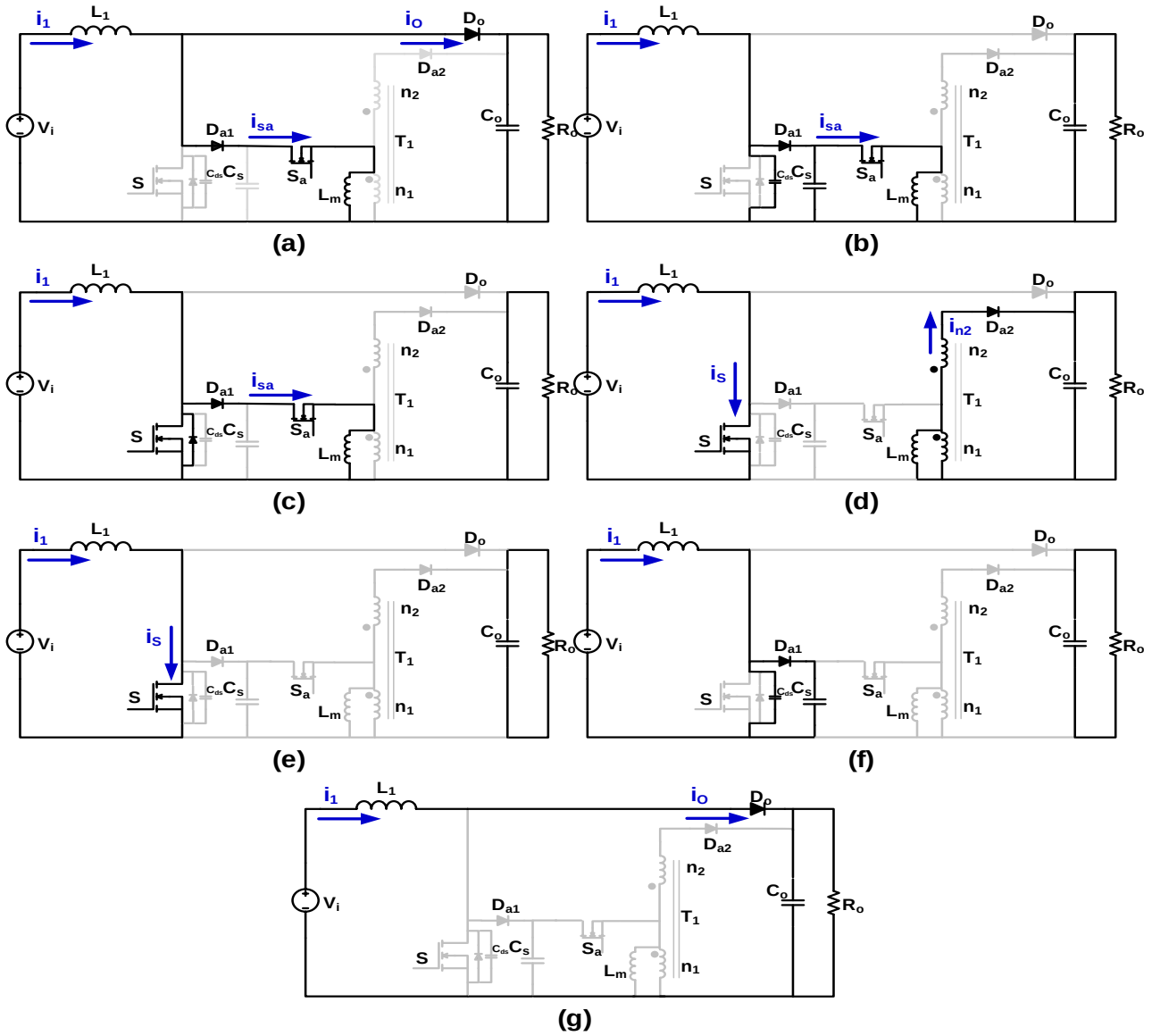

Fig. 2: The equivalent configurations of the proposed converter at operating subintervals (a) Status1, (b) Status2, (c) Status3, (d) Status4, (e) Status5, (f) Status6, (g) Status7.

zero. Under ZCS conditions, the output diode D_o turns off, and the following status begins. The corresponding configuration of this status is depicted in Fig. 2a. The equations of this mode are derived as:

$$i_m = i_{sa} = \frac{V_o}{L_m}(t - t_0) \quad (1)$$

$$v_{cs} = V_o \quad (2)$$

L_m represents the magnetizing inductance of T_1, and V_o is the output voltage.

This is how the duration of this mode is expressed:

$$\Delta t_1 = \frac{I_b L_m}{V_o} \quad (3)$$

Status 2 [t1, t2]: When the output diode turns off, this subinterval starts. The magnetizing inductor L_m and the resonant capacitor C_s combine to create a resonant circuit. In a resonance, as depicted in Fig. 3, the voltage of the capacitor C_s starts to fall from the output voltage to zero. When the voltage of the resonant capacitor is fully depleted, this status is finished. The corresponding configuration of this state is depicted in Fig. 2b. The voltage of the capacitor C_s and the current passes through the auxiliary switch S_a are calculated using the following equations.

$$v_{cs} = V_o \cos(\omega_2(t - t_1)) \quad (4)$$

$$i_{sa} = i_m = I_b + V_o\sqrt{\frac{C_s}{L_m}}\sin(\omega_2(t - t_1)) \quad (5)$$

where ω_2 is the status 2 auxiliary circuit resonance frequency.

The duration of this status can be obtained as follows:

$$\Delta t_2 = \pi\sqrt{C_s L_m} \quad (6)$$

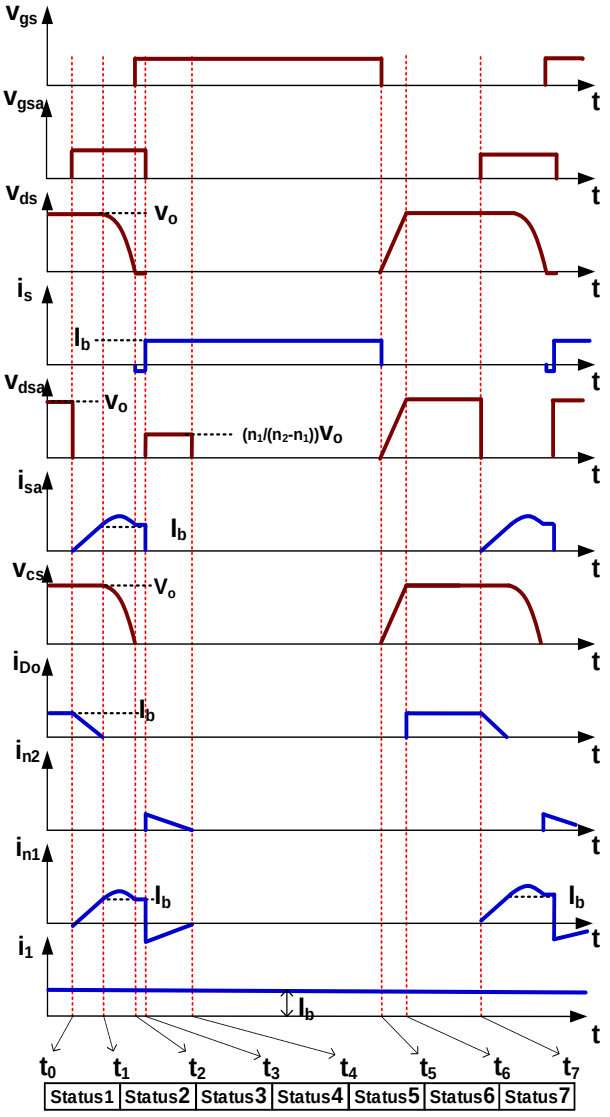

Fig. 3: The key waveforms of the proposed active snubber cell boost converter.

Status 3 [t2, t3]: The main switch S turns on at the start of this mode. Moreover, the input auxiliary diode D_{a1} and the anti-parallel diode of the main switch are conducting. Fig. 2c depicts the equivalent circuit of this mode. The time duration of this subinterval is short and negligible. At the end of this mode, the current flowing through the auxiliary diode D_{a1} and the switch's body diode are zero, and the auxiliary switch Sa is off with zero current flowing through it. The main switch and input inductance function as a straightforward boost circuit at the mode's conclusion, while the coupled inductors discharge the energy stored to the output similar to the flyback circuit.

Status 4 [t3, t4]: At the start of this status, the auxiliary switch S_a is off. The windings n_1, n_2, and the output auxiliary diode D_{a2} discharge the energy held in the magnetizing inductor L_m. The auxiliary switch turns off at practically ZVS condition by choosing the appropriate turns ratio for the coupled inductors. The primary switch S also carries the input current I_b. The equivalent circuit of this status is shown in Fig. 2d. At the end of this status, the auxiliary diode D_{a2} turns off and the energy stored in the magnetizing inductor L_m is fully discharged. The voltages across the windings n_1 and n_2 and the currents flowing through the winding n_2 and the output auxiliary diode D_{a2} are stated as follows:

$$i_{n2} = i_{D_{a2}} = \frac{n_1}{n_2 - n_1} I_b \tag{7}$$

$$v_{n1} = \frac{n_1}{n_1 - n_2} V_o \tag{8}$$

$$v_{n2} = \frac{n_2}{n_1 - n_2} V_o \tag{9}$$

where n_1 is the primary and n_2 is the secondary winding of the coupled inductor T1.

Following is the description of timeframe for this status:

$$\Delta t_4 = \left(\frac{n_2 - n_1}{n_1} \right) \frac{L_m I_b}{V_o} \tag{10}$$

Status 5 [t4, t5]: In this state, the primary switch S is conducting, the output diode of the boost converter is off, and the magnetizing inductances of coupled inductors are fully discharged in this state. The corresponding configuration of this state is shown in Fig. 2e. This condition is comparable to the typical boost converter.

Status 6 [t5, t6]: The main switch S does not conduct at the start of this condition. The input current i_1 parallels the parasitic drain-source capacitance C_{ds} of the main switch by passing via the resonant capacitors C_s. As a result, under ZVS conditions, the voltage of the primary switch rises linearly, and the switch turns off. The output diode turns on under ZVS when the voltage of the main switch reaches the output voltage. The voltage of the resonant capacitor and the voltage of the main switch are thereby constrained to the output voltage. The equivalent configuration of this status is shown in Fig. 2f. Following is the equation for this status:

$$v_{C_s} = v_{ds} = v_{dsa} = \frac{I_b}{C_s}(t - t_5) \tag{11}$$

which the period of this mode is derived as follows:

$$\Delta t_6 = C_s \frac{V_o}{I_b} \tag{12}$$

Status 7 [t6, t7]: The input inductor is being discharged at the start of this condition, and the output diode D_o becomes forward-biased. The suggested converter functions similarly to a standard boost converter in this state. The corresponding configuration of this state is shown in Fig. 2g.

Simulation Results

To verify the performance of the proposed active

snubber cell and compare the experimental results with simulation results, the waveforms of the proposed converter are extracted. The gate commands of switches and the voltage of the resonance capacitor and main switches are shown in Fig. 4(a), and it can be seen the main switch turns on just after its voltage reaches zero by resonance occurring between the resonance and body capacitor of the main switch and magnetizing inductance.

The voltage and current waveforms of the main switch are shown in Fig. 4(b).

Moreover, to monitor the performance of the auxiliary switch, its current and voltage waveform are illustrated in Fig. 4(c), and the input and output current of the coupled inductor are depicted in Fig. 4(d) by measuring the current of the auxiliary switch S_a and current of the auxiliary diode D_{a2}.

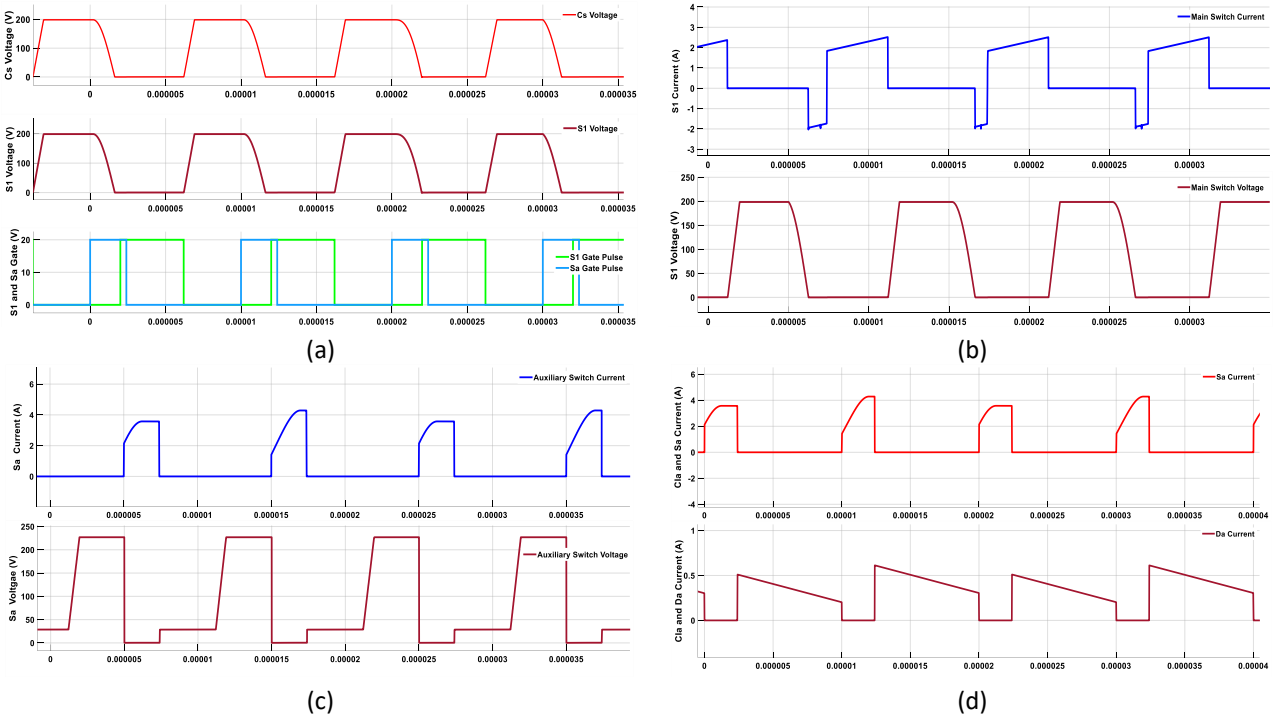

Fig. 4: A 200 W simulation result of the suggested active snubber cell, (a) the gate commands of switches and resonance and main switch voltage, (b) the main switch's voltage and current, (c) the auxiliary switch's voltage and current, (d) measured current of coupled inductors which passed the auxiliary snubber switch and the auxiliary output diode.

Stresses Analysis of the Proposed Converter

At the end of status 6, the peak voltage across the switches S, S_a, and can be calculated as follows:

$$v_S = V_o \tag{13}$$

$$v_{sa} = \left(\frac{n_1}{n_2 - n_1}\right) Vo \tag{14}$$

The voltage stress across S_a is equal to V_o and the peak current passes through the main switch S can be determined as follow:

$$i_S = \frac{P_{out}}{V_{in}} + \frac{\Delta I}{2} \tag{15}$$

Where ΔI is the current ripple of the input inductor I_b.

Also, the peak current which passes through the auxiliary switch is obtained from mode 2:

$$i_{Sa} = I_b + V_o \sqrt{\frac{C_s}{L_m}} \tag{16}$$

The voltage and current stresses of the main diode D_o is calculated as follows:

$$v_{D_o} = V_o \tag{17}$$

$$i_{D_o} = \frac{P_{out}}{V_{in}} + \frac{\Delta I}{2} \tag{18}$$

The voltage stress and the current peak of the input and output auxiliary diodes D_{a1}, D_{a2} are calculated using:

$$v_{D_{a2}} = \frac{n_2}{n_1} V_o \tag{19}$$

$$v_{D_{a1}} \cong 0 \tag{20}$$

$$i_{D_{a1}} = I_b + V_o \sqrt{\frac{C_s}{L_m}} \tag{21}$$

$$i_{D_{a2}} = \frac{n_1}{n_2 - n_1} I_b \tag{22}$$

Design Method

When the input current I_b at the end of status 1 exceeds the current flowing through magnetizing inductance of the coupled inductor T_1, the main switch S is in the soft-switching condition. As a result, as long as the following equation is established, the main switch works under soft-switching conditions:

$$I_b < i_m(t_1) = \frac{V_o}{L_m}\Delta t_1 \quad (23)$$

Where the Δt_1 is obtained from (3).
By considering $i_m(t1)$ 15% higher than I_b, the following relation is obtained:

$$1.15 I_b = \frac{V_o}{L_m}\Delta t_1 \quad (24)$$

Additionally, compared to the main switching cycle, the operating time of the auxiliary circuit must be insignificant. This duration is therefore chosen to be ten times shorter than the switching period.

$$\Delta t_1 + \Delta t_2 + \Delta t_4 + \Delta t_6 = \frac{T_{switching}}{10} \quad (25)$$

Where $\Delta t_i : i = 1,2,4,6$ are the time duration of statuses 1, 2, 4, and 6 and are given from (3), (6), (10), and (12) and $T_{switching}$ is the switching cycle of the proposed converter.

From (24), the inductance L_m is calculated by taking into consideration a specific value for the time duration. The ratio between the peak current of the auxiliary switch and the main switch is used to determine the value of the resonant capacitor Cs.

$$\left(\frac{I_{sa}}{I_s}\right)_{peak} = 1 + \frac{V_o}{I_b}\sqrt{\frac{C_s}{L_m}} = \lambda \quad (26)$$

The longer the time period for λ is obtained, the larger the value for Δt_2 is. The turn ratio of the primary winding of coupled inductor depends on the value of the inductance L_m. The minimum voltage stress on the auxiliary components S_a and D_{a2} is used to calculate the turns ratio $n_1 : n_2$ of the coupled inductor. The condition (26) should be examined following the design of the resonant capacitor C_s and the magnetizing inductance L_m. The equations in "Stresses analysis of the proposed converter" section is used to choose all active components. Similar to a traditional PWM boost converter, the values for L_b and C_o are obtained based on the desired current and voltage ripple.
Furthermore, to compare the proposed snubber cell with its counterparts in terms of voltage gain, output power, switching frequency, efficiency, and component counts, such as the number of auxiliary switches and diode, capacitor, inductor, and coupled inductors, a comprehensive comparison is made, and the results are presented in Table 1.

Experimental Results

A 200 W implementation with supply voltage of 90 V, output voltage of 200 V, and switching frequency of 100 kHz has been constructed and evaluated to corroborate the findings of the theoretical analysis of the suggested circuit. The experimental specifications for this converter are shown in Table 2, and the actual converter's circuit. The experimental specifications for this converter are shown in Table 2, and the actual converter's circuit schematic is shown in Fig. 7. The magnetizing inductance L_m 100 uH and the resonant capacitor C_s 10 nF are both meant for the auxiliary circuit. The linked inductor is also selected with a 2:16 turns ratio. The input inductor is set to have a value of 400 uH in the interim.

Table 1: proposed converter and its counterpart's comparison

Refs	Efficiency [%]	Experimental Parameters			Number of Auxiliary components				
		V_{out}/V_{in}	P_{out} [W]	f_{sw} [kHz]	Switch	Diode	C	L	Coupled Ind.
[12], [13]	96.23	2.67	600	30	1	2	2	2	0
[16]	96	2	200	100	0	4	1	3	0
[17]	97	1.5	300	180	0	2	2	1	0
[20]	93.9	-	300	20	1	4	2	2	1
[23]	>97	1.07	1200	80	1	1	2	1	0
[24]	98	1.29	1000	100	1	4	2	2	0
[25]	96	1.6	2000	30	2	2	1	0	0
[27]	97	2	100	100	0	3	1	3	0
[30]	98.28	2	200	32.2	1	3	1	1	0
Proposed	95.9	2.2	200	100	1	2	1	0	1

Table 2: The parameters of the experimental prototype

Description	Symbol	Value
Input Voltage	V_{in}	90 V
Output Voltage	V_O	200 V
Max. Output Power	P_O	200 W
Frequency of main switch	f_s	100 kHz
Frequency of auxiliary switch	f_{sa}	100 kHz
Input Inductor	L_1	400 uH
Resonance Capacitor	C_s	10 nF
Magnetizing Inductance	L_m	100 uH
Output Capacitor	C_O	100 uF
Coupled Inductor Core	T_1	E34/14/9
Turn Ratio of CI	n1/n2	2/16

Fig. 5a shows the experimental voltage and current of the primary switch. The primary switch turns on under ZVS conditions, and switches off under ZCS situations. As previously mentioned, the snubber circuit also prevents any voltage or current strains from being applied to the primary switch. Fig. 5b displays the auxiliary switch's voltage and current.

As can be observed, the auxiliary switch has an output voltage-equivalent voltage stress, operates under ZCS, and shuts off with low switching losses. Additionally, the peak current of the auxiliary switch is a little bit higher than that of the main switch.

The charge and discharge situation of the resonant capacitor in terms of voltage to achieve the soft switching condition are shown in Fig. 5c. Fig. 5d demonstrates the waveforms of coupled inductors, where the core is charged first, then is discharged when the auxiliary switch is turned off.

To depict the volume and dimensions of this converter, the implemented prototype of the proposed circuit is shown in Fig. 6.

Furthermore, the part number of all active devices and the values of passive devices are noted and presented in Fig. 7.

In Fig. 8, the measured efficiency of this converter is provided. The nominal load of 200 W yields a maximum efficiency of 95.9%, an increase of 6.3% in efficiency over a traditional boost converter.

Notably, all circumstances, including input voltage, switching frequency, and voltage gain, are considered the same for a fair comparison of the efficiency between this article and the conventional boost converter.

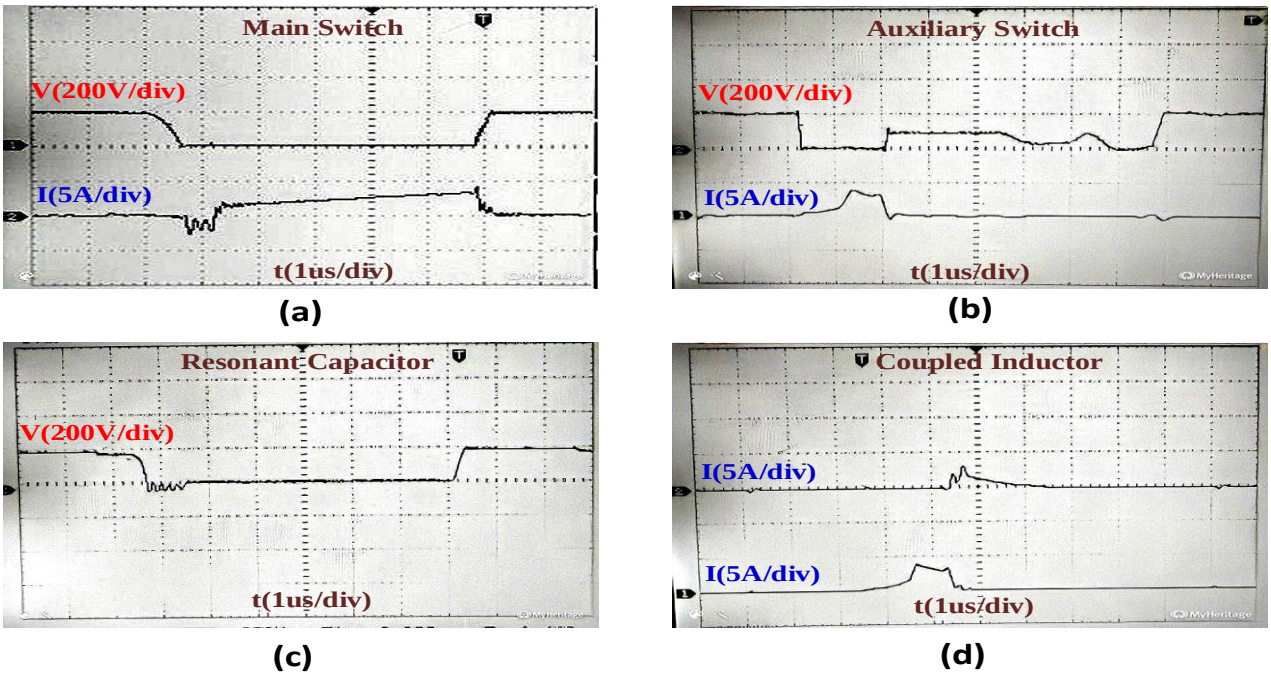

Fig. 5: A 200 W experimental result of the suggested active snubber cell, (a) the main switch's voltage and current, (b) the auxiliary switch's voltage and current, (c) voltage of resonant capacitor, (d) measured current of coupled inductors which passed the auxiliary snubber switch and the auxiliary output diode.

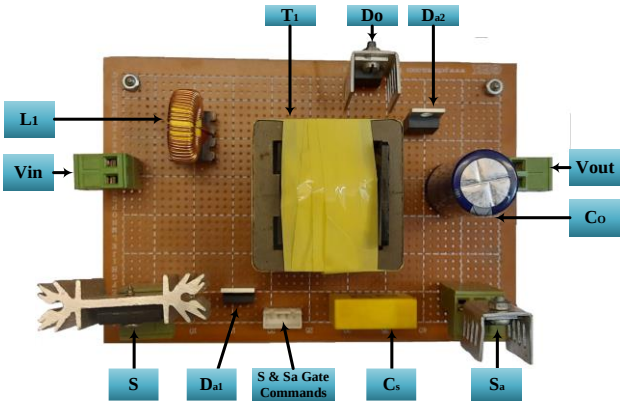

Fig. 6: The implemented figure of the suggested circuit.

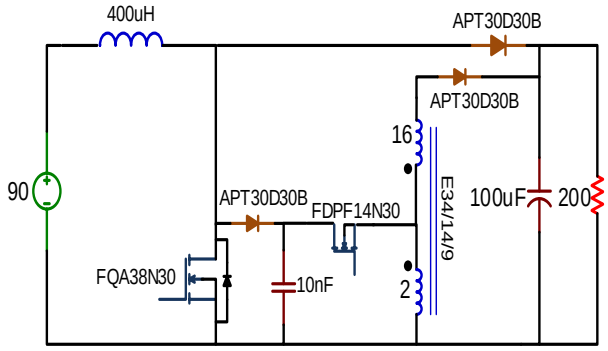

Fig. 7: Parameters of the implemented prototype.

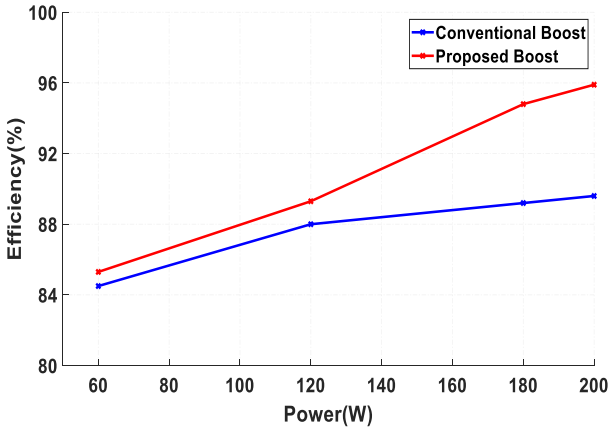

Fig. 8: The measure efficiency of the proposed converter.

Conclusion

This paper provides a new low-stress soft-switching boost converter using a simple coupled-inductor in the auxiliary circuit. Moreover, the auxiliary part consists of two diodes, one switch, one resonance capacitor, and a coupled inductor. The suggested auxiliary circuit provides soft switching condition for the main switch, which provides ZVS in turn-on transient and ZCS in turn-off transient, while in this situation, the soft-switching condition is provided for the auxiliary switch in which turns on under ZCS and also turns off with practically ZVS conditions. The auxiliary circuit does not impose additional voltage or current stress to the main switch. A 200 W prototype is implemented to validate the performance of this snubber cell. The experimental data reported here support the theoretical analysis. The best point of efficiency is 95.9% which is occurred at maximum load, and is 6.3% greater than the traditional counterparts. The number of components in this topology is more efficient than other counterparts. Still, the auxiliary switch, a high-side switch, could be considered one of the main challenging issues in this topology. On the other hand, this auxiliary switch operates under ZCS, which is suitable for IGBT switches, not MOSFET.

Author Contributions

Mohammad Ali Latifzadeh in collaboration with Hesamodin Allahyari and Hadi Faezi, designed, simulated, carried out the data analysis, implemented the prototype and wrote the manuscript thoroughly under supervising of dr. Parviz Amiri.

Acknowledgment

The editors of JECEI and the anonymous reviewers are sincerely appreciated for their insightful criticism and recommendations, which the authors acknowledge in advance.

Conflict of Interest

Regarding the publishing of this study, the authors state that there are no possible conflicts of interest. The authors have also fully observed all ethical difficulties, such as plagiarism, informed consent, misconduct, data fabrication or falsification, duplicate publishing or submission, and redundancy.

Abbreviations

ZVT	Zero Voltage Transient
ZVS	Zero Voltage Switching
ZCS	Zero Current Switching
PWM	Pulse Width Modulation
EMI	Electro-Magnetic Interference
CIs	Coupled Inductors

References

[1] H. Soltani Gohari, K. Abbaszadeh, "Bidirectional Buck-Boost integrated converter for plug-in hybrid electric vehicles," J. Electr. Comput. Eng. Innovations (JECEI), 8(1): 109-124, 2020.

[2] P. Amiri, M. Sharafi, "A high efficiency low-voltage soft switching DC–DC converter for portable applications," J. Electr. Comput. Eng. Innovations (JECEI), 1(2): 73-81, 2013.

[3] V. K. Goyal, A. Shukla, "Isolated DC–DC boost converter for wide input voltage range and wide load range applications," IEEE Trans. Ind. Electron., 68(10): 9527-9539, 2021.

[4] A. Shoaei, K. Abbaszadeh, H. Allahyari, "A single-inductor multi-input multi-level high step-up DC-DC converter based on switched-diode-capacitor cells for PV applications," IEEE J. Emerging Sel. Top. Ind. Electron., 4(1): 18-27, 2022.

[5] R. S. Inomoto, J. R. B. A. Monteiro, A. J. Sguarezi Filho, "Boost converter control of PV system using sliding mode control with integrative sliding surface," IEEE J. Emerging Sel. Top. Power Electron., 10(5): 5522-5530, 2022.

[6] F. M. Shahir, E. Babaei, M. Farsadi, "Extended topology for a boost DC–DC Converter," IEEE Trans. Power Electron., 34(3): 2375-2384, 2019.

[7] N. Molavi, E. Adib, H. Farzanehfard, "Soft-switched non-isolated high step-up DC–DC converter with reduced voltage stress," IET Power Electron., 9(8): 1711-1718, 2016.

[8] H. Bahrami, H. Iman-Eini, B. Kazemi, A. Taheri, "Modified step-up boost converter with coupled-inductor and super-lift techniques," IET Power Electron., 8(6): 898-905, 2015.

[9] M. Delzendeh Sarfejo, H. Allahyari, H. Bahrami, A. Afifi, M. Latif Zadeh, E. Yavari, M. Ghavidel Jalise, "A passive compensator for imbalances in current sharing of parallel-SiC MOSFETs based on planar transformer," IET Power Electron., 14(14): 2400-2412, 2021.

[10] M. Nikbakht, S. Abbasian, M. Farsijani, K. Abbaszadeh, "An ultra high gain double switch quadratic boost coupled inductor based converter," in Proc. 2022 13th Power Electronics, Drive Systems, and Technologies Conference (PEDSTC): 167-172, 2022.

[11] M. Fazeli-Hasanabadi, A. Shoaei, K. Abbaszadeh, H. Allahyari, "An interleaved high step-up dual-input single-output DC-DC converter for electric vehicles," in Proc. 2022 13th Power Electronics, Drive Systems, and Technologies Conference (PEDSTC): 145-149, 2022.

[12] F. Falahi, E. Babaei, S. Bagheri, "Soft-switched interleaved high step-up non-isolated DC-DC converter with high voltage gain ratio," in Proc. 2022 13th Power Electronics, Drive Systems, and Technologies Conference (PEDSTC): 128-133, 2022.

[13] S. Park, G. Cha, Y. Jung, C. Won, "Design and application for PV generation system using a soft-switching boost converter with SARC", IEEE Trans. Ind. Electron., 57(2): 515-522, 2010.

[14] H. Bahrami, H. Allahyari, E. Adib, "An improved wide ZVS soft-switching range PWM bidirectional forward converter for low power applications with simple control circuit," IET Power Electron., 15(15): 1652-1663, 2022.

[15] H. Bahrami, H. Allahyari, E. Adib, "A self-driven synchronous rectification ZCS PWM two-switch forward converter with minimum number of components," IEEE Trans. Ind. Electron., 69(12): 12842-12850, 2022.

[16] M. Mohammadi, E. Adib, M. R. Yazdani, "Family of soft-switching single-switch PWM converters with lossless passive snubber," IEEE Trans. Ind. Electron., 62(6): 3473-3481, 2015.

[17] H. Choe, Y. Chung, C. Sung, J. Yun, B. Kang, "Passive snubber for reducing switching-power losses of an IGBT in a DC–DC boost converter," IEEE Trans. Power Electron., 29(12): 6332-6341, 2014.

[18] T. Zhan, Y. Zhang, J. Nie, Y. Zhang, Z. Zhao, "A novel soft-switching boost converter with magnetically coupled resonant snubber," IEEE Trans. Power Electron., 29(11): 5680-5687, 2014.

[19] M. T. Kejani, S. H. Aleyasin, A. Safaeinasab, K. Abbaszadeh, "A new non-isolated single switch high step-up DC/DC converter based on inductor cells," in Proc. 2021 12th Power Electronics, Drive Systems, and Technologies Conference (PEDSTC): 1-5, 2021.

[20] W. Qian, X. Zhang, Z. Li, "Design and operation analysis of a novel coupled-inductor based soft switching boost converter with an auxiliary switch," in Proc. 2016 IEEE 8th Int. Power Electron. and Motion Control Conf. (IPEMC-ECCE Asia): 2534-2537, Hefei, 2016.

[21] M. Ghavidel Jalise, H. Allahyari, A. Shoaei, E. Adib, H. Bahrami, M. A. Latif Zadeh, M. H. Fahimifar, "A self-driven synchronous rectification wide-range ZVS single-switch forward converter controlled using the variable inductance," IET Power Electron., 16(2): 320-332, 2022.

[22] H. Bahrami, E. Adib, S. Farhangi, H. Iman-Eini, R. Golmohammadi, "ZCS-PWM interleaved boost converter using resonance-clamp auxiliary circuit," IET Power Electron., 10(3): 405-412, 2017.

[23] Y. Jang, M. M. Jovanovic, "A new, soft-switched, high-power factor boost converter with IGBTs," IEEE Trans. Power Electron.,17(4): 469-476, 2002.

[24] S. Cetin, "Power-Factor-Corrected and fully soft-switched pwm boost converter," IEEE Trans. Ind. Appl., 54(4): 3508-3517, 2018.

[25] J. Bauman, M. Kazerani, "A novel capacitor-switched regenerative snubber for DC/DC boost converters," IEEE Trans. Ind. Electron., 58(2): 514-523, 2011.

[26] Y. Chen, Z. Li, R. Liang, "A novel soft-switching interleaved coupled-inductor boost converter with only single auxiliary circuit," IEEE Trans. Power Electron., 33(3): 2267-2281, 2018.

[27] J. A. Lambert, J. B. Vieira, L. Carlos de Freitas, L. dos Reis Barbosa, V. J. Farias, "A boost PWM soft-single-switched converter with low voltage and current stresses," IEEE Trans. Power Electron., 13(1): 26-35, 1998.

[28] N. Ting, I. Aksoy, Y. Sahin, "ZVT-PWM DC–DC boost converter with active snubber cell," IET Power Electron., 10(2): 251-260, 2017.

[29] C. Wang, C. Lin, C. Lu, J. Li, "Analysis, design, and realisation of a ZVT interleaved boost DC/DC converter with single ZVT auxiliary circuit," IET Power Electron., 10(14): 1789-1799, 2017.

[30] A. Mondzik, R. Stala, S. Piróg, A. Penczek, P. Gucwa, M. Szarek, "High efficiency DC–DC boost converter with passive snubber and reduced switching losses," IEEE Trans. Ind. Electron., 69(3): 2500-2510, 2022.

Biographies



Mohamad Ali Latifzadeh received his B.Sc. degree in electrical engineering from Malek Ashtar University of Technology, Isfahan, Iran, in 2002, and the M.Sc. degree in electrical engineering from the Malek Ashtar University of Technology, Tehran, Iran, in 2007 and PhD degree in electrical engineering from the Malek Ashtar University of Technology Tehran, Iran, in 2018. His research interests include design, modeling in DSP embedded module, tracking, mono-pulse tracking and satellite ground station systems.

- Email: mal_1358@yahoo.com
- ORCID: 0009-0001-6909-6261
- Web of Science Researcher ID: NA
- Scopus Author ID: 57258099200
- Homepage: NA



Parviz Amiri was born in 1970. He received his B.Sc. degree from university of Mazandaran 1994, the M.Sc. from Khaje Nasir toosi University (KNTU Tehran, Iran) in 1997, and his Ph.D. from University of Tarbiat Modares (TMU Tehran, Iran) in 2010, all degrees in Electrical Engineering (Electronics). His main research includes electronic circuit design in industries. His primary research interest is in RF and power electronics circuits, with focus on highly efficient and high linear power circuit design. He is currently with the Faculty of Electrical and Computer Engineering at Shahid Rajaee teacher Training University in Tehran, Iran.

- Email: pamiri@sru.ac.ir
- ORCID: 0009-0001-6909-6261
- Web of Science Researcher ID: NA
- Scopus Author ID: 57258099200
- Homepage: NA



Hesamodin Allahyari was born in Tehran, Iran, in 1994. He received the B.Sc. degree in electrical engineering from Shahid Beheshti University, Tehran, Iran, in 2017, and the M.Sc. degree in electrical engineering from the K.N. Toosi University of Technology, Tehran, Iran, in 2020. He is currently with High Voltage Power Electronics Laboratory, K.N. Toosi University of Technology, Tehran, Iran. His research interests include dc–dc power converter, resonant converter, and pulse power supplies.

• Email: h.allahyari@email.kntu.ac.ir
• ORCID: 0000-0002-7098-6456
• Web of Science Researcher ID: ABD-3635-2021
• Scopus Author ID: 57257874800
• Homepage: NA

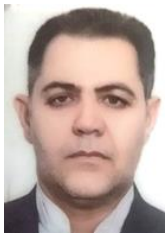

Hadi Faezi was born in Sabzevar, Iran, in 1977. He received the B.Sc. degree in electrical engineering from Malek Ashtar University of Technology, Isfahan, Iran, in 2000, and the M.Sc. degree in electrical engineering from the School of Electrical and Computer Engineering, College of Engineering, University of Tehran, Tehran, Iran, in 2003 and the PhD degree in electrical engineering from the Iran University of Science and Technology (IUST), Tehran, Iran, in 2019. His research interests include Microwave, antennas and electromagnetic radiation, pulsed power supplies and power converters.

• Email: faezi@mut.ac.ir
• ORCID: 0000-0002-6303-3454
• Web of Science Researcher ID: HNS-9988-2023
• Scopus Author ID: 24724346300
• Homepage: NA

How to cite this paper:
M. A. Latifzadeh, P. Amiri, H. Allahyari, H. Faezi "A new low-stress soft-switching boost converter using coupled-inductor active auxiliary circuit" J. Electr. Comput. Eng. Innovations, 11(2): 433-442, 2023.

DOI: 10.22061/jecei.2023.9304.607

URL: https://jecei.sru.ac.ir/article_1878.html